Eur. Phys. J. A **11**, 413–420 (2001)

THE EUROPEAN PHYSICAL JOURNAL A

High-precision measurement of the ^{14}O half-life using a mass-separated radioactive beam

M. Gaelens[a], J. Andrzejewski[b], J. Camps, P. Decrock, M. Huyse, K. Kruglov, W.F. Mueller[c], A. Piechaczek[d], N. Severijns[e], J. Szerypo[f], G. Vancraeynest, P. Van Duppen, and J. Wauters

Instituut voor Kern- en Stralingsfysica, Katholieke Universiteit Leuven, Celestijnenlaan 200 D, B-3001 Leuven, Belgium

Received: 5 April 2001 / Revised version: 6 August 2001
Communicated by J. Äystö

Abstract. A high-precision measurement of the ^{14}O half-life has been performed using a mass-separated radioactive beam in combination with a germanium detector set-up. This is the first ^{14}O half-life measurement with a contamination-free source. The final result of 70.560 ± 0.049 seconds is in agreement with the generally adopted mean value.

PACS. 23.40.-s Beta decay; double beta decay; electron and muon capture – 29.25.Ni Ion sources: positive and negative – 29.25.Rm Sources of radioactive nuclei

1 Introduction

The precise determination of the ft-value of superallowed $0^+ \rightarrow 0^+$ pure Fermi β transitions is important in validating the electroweak interaction theory. The average ft-value of these transitions serves as a test for the Conserved Vector Current hypothesis, for the determination of the vector coupling constant $G_{\rm V}$ of nuclear β decay and for the adequacy of the three-generation Standard Model, *i.e.* the determination of the V_{ud} element of the Cabibbo-Kobayashi-Maskawa (CKM) quark mixing matrix. Currently, nine transitions have been measured to a precision better than $2{\cdot}10^{-3}$: ^{10}C, ^{14}O, ^{26}Al$^{\rm m}$, ^{34}Cl, ^{38}K$^{\rm m}$, ^{42}Sc, ^{46}V, ^{50}Mn and ^{54}Co [1,2]. Whereas the analysis of the presently available data set confirms the CVC hypothesis at the $3 \cdot 10^{-4}$ precision level, the unitarity test, based on the extracted value of V_{ud}, points to a 2.2 σ deviation from the Standard Model [2]. The matrix element V_{ud} can also be determined from the decay of the free neutron. A recent analysis of the world data on neutron decay yielded a value of V_{ud} in agreement with unitarity [2]. However, if one considers only the most recent and also most precise result for the electron asymmetry [3], a value for V_{ud} which deviates 2.7 σ from the Standard Model is obtained, the deviation being in the same direction as in the case of the $0^+ \rightarrow 0^+$ transitions.

From the above it is clear that the current situation with respect to the unitarity test of the CKM matrix is far from satisfactory. In high-energy physics, the other matrix element which is important for this unitarity test, *i.e.* V_{ub}, is currently addressed again, as well experimentally as theoretically [4]. As for V_{ud} , which can only be determined with high precision in β decay, a continued effort is needed in order to improve, and at the same time extend to higher masses, both the necessary theoretical calculations of the isospin and nuclear-structure corrections, as well as the experimental input data, *i.e.* $Q_{\rm EC}$-values, half-lives and branching ratios.

Several results on the half-life of ^{14}O were reported already. The existing data set was evaluated by Hardy *et al.* [1] and also by Wilkinson [5] to extract the best measurements with the highest accuracy. Five high-precision measurements exist [6–10]. The weighted average of these is 70.603 ± 0.018 s with $\chi^2/\nu = 0.815$ and a confidence level of 53%. All five measurements underwent extensive searches for possible systematic errors in measurement and analysis. However, because they were performed in-beam, *i.e.* the detectors faced the irradiated target, all have one possible remaining cause for error in common, namely contamination of the sample produced via the different reaction channels. Although the main contaminants ^{15}O, ^{13}N and ^{11}C of the reaction ^{12}C(^{3}He, n)^{14}O, used in all experiments, do not emit characteristic γ-rays, they can influence the γ spectrum with annihilation radiation, de-

[a] *Present address*: Centre de Recherches du Cyclotron, Chemin du Cyclotron 2, B-1348 Louvain-la-Neuve, Belgium.
[b] *Present address*: University of Lodz, Lodz, Poland.
[c] *Present address*: NSCL, Michigan State University, East-Lansing, USA.
[d] *Present address*: Louisiana State University, Baton Rouge, USA.
[e] e-mail: `Nathal.Severijns@fys.kuleuven.ac.be`
[f] *Present address*: Department of Phyics, University of Jyvaskyla, Finland.

cay positrons and their bremsstrahlung. Thus, even when using germanium detector arrays, whereby specific γ-rays are selected, the contaminating activity can still influence the dead-time and pile-up correction procedures. Becker *et al.* [8] calculated that contamination of the ^{14}O source with an activity with half the half-life could result in an undetected error (meaning that there is no influence of the contamination on the χ^2 of the half-life fit) of 0.2% when the ^{14}O decay is measured for five half-lives with total statistics of 10^7 counts. Noting that the desired accuracy is about $5 \cdot 10^{-4}$ it must be clear that this contamination problem is indeed serious in high-precision measurements.

A new high-precision half-life measurement on ^{14}O was therefore undertaken in an environment potentially free of contamination. Earlier development work on targets and ion sources for the production of radioactive beams [11, 12] together with the integration of this equipment on the LISOL mass separator [13,14] allowed for the first time the production of a mass-separated ^{14}O radioactive source. Moreover, since the experimental set-up used in this work is very different from those used in earlier measurements of the ^{14}O half-life, some of the systematic uncertainties arise from very different factors.

2 Experimental

2.1 Production and purity of ^{14}O beam

The ^{14}O isotopes were produced in the ^{12}C(^{3}He, n)^{14}O reaction using a 36 MeV ^{3}He^{1+} primary beam from the CYCLONE cyclotron with maximum intensity of 5 μA, bombarding a natural carbon target (graphite). The radioactive atoms were mass separated with the Leuven Isotope Separator On-Line (LISOL). A Forced Electron Beam Induced Arc Discharge (FEBIAD) ion source with an internal graphite target [15] was used. The total efficiency was about $4 \cdot 10^{-3}$. The ^{14}O used in the experiment was extracted as a ^{12}C^{14}O^{1+} beam. Maximum extracted beam intensities on this molecular fraction yielded $2.3 \cdot 10^5$ ^{12}C^{14}O ions/μC. The ratio between the atomic ^{14}O (mass 14) beam and the molecular ^{12}C^{14}O (mass 26) beam was 0.12.

During the production process different radioactive isotopes were produced. Besides ^{14}O, produced via the ^{12}C(^{3}He, n) reaction, ^{13}N was produced via ^{12}C(^{3}He, pn) or ^{12}C(^{3}He, d) reactions, ^{15}O via ^{13}C(^{3}He, p) and ^{11}C via ^{12}C(^{3}He, α). By using mass separation, contaminating activity could be reduced strongly. However, since the molecular sideband of ^{12}C^{14}O was used instead of the ^{14}O beam, some contamination could still be possible. The contamination of the mass 26 molecules ^{13}N^{13}N and ^{11}C^{15}O was at the level of 10^{-7} [11], which can be neglected. A second possible and more important cause of contamination is the tail of mass 27 (^{13}N^{14}N) under mass 26. This was investigated by taking a mass scan and extrapolating the mass 27 contribution under the mass 26 peak. From this, the resulting contamination level was estimated to be about 10^{-3} or less. The time behavior of the detected γ-rays did not show any sign of the presence of ^{13}N at mass 26.

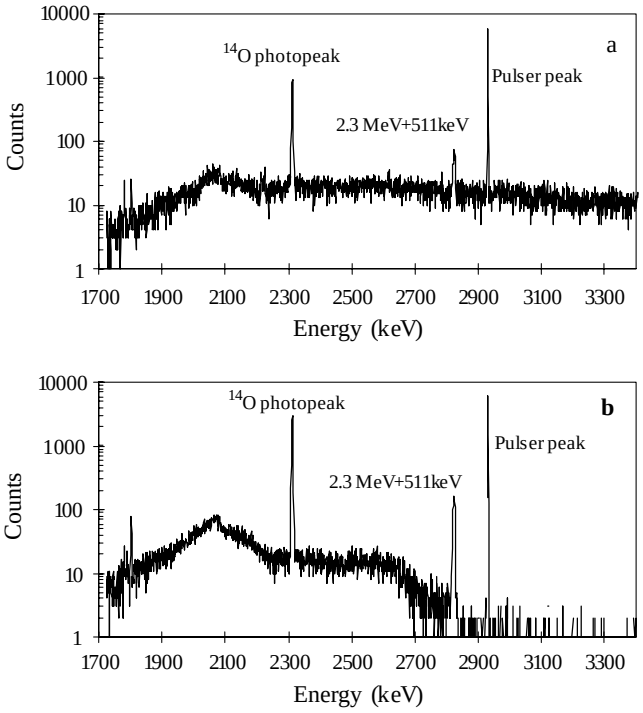

Fig. 1. Comparison of energy spectra obtained: a) during a test run when cyclotron and separator beam were on during the decay measurement, *i.e.* while the decay was measured, a new source was prepared at the implantation station, and b) during the actual measurement, *i.e.* when the cyclotron beam was switched off, showing the strong reduction in background. The spectrum in b) has about 3 times more counts in the 2.3 MeV photopeak compared to the spectrum in a).

The half-life of ^{14}O was determined by the time behavior of the 2.313 MeV γ-ray of the ^{14}O decay. Therefore, since the contaminants ^{15}O, ^{13}N and ^{11}C do not emit γ-rays and were only visible in the spectrum by their 511 keV annihilation radiation and the β^+ particle bremsstrahlung, the way they interfered with our measurement was by affecting the total count rate in the detector. This total count rate was used for the dead-time correction and, as will be shown later, a contamination level of a few % would have a clear influence on the final result. However, as was mentioned before, all possible contamination was below the 0.1% level.

2.2 Experimental set-up

The mass-separated beam was implanted in an aluminized mylar tape which was thereafter moved towards the decay station, thereby also removing any remaining activity from previous implantations from this decay station.

The detection system consisted of two germanium detectors with relative efficiency of 70% and 75% for the 1.332 MeV γ line of ^{60}Co with respect to a 3 inch by 3 inch NaI crystal taken at a source-to-detector distance of 25 cm. Their energy resolution was typically 2.2 keV at 1.332 MeV. The detectors were mounted in a lead cylinder which encapsulated the end-cap of the detector. This

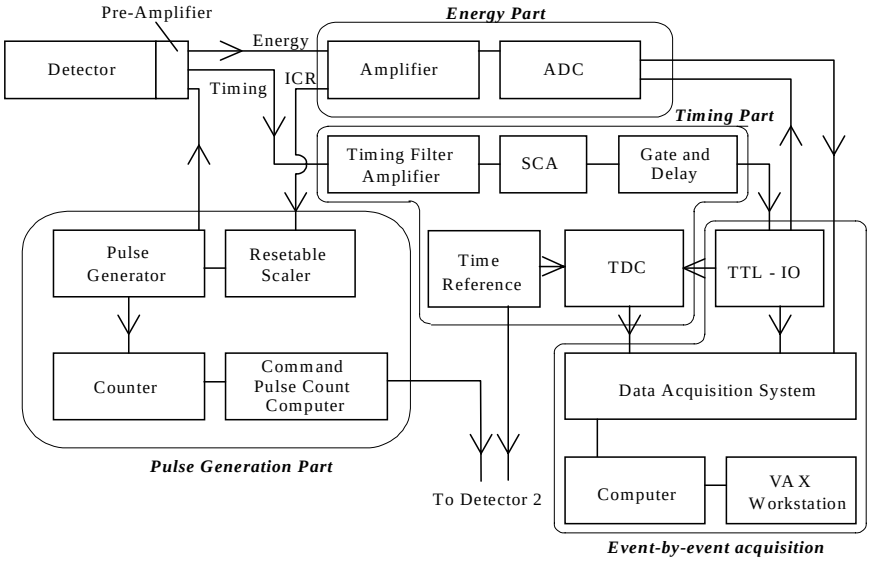

Fig. 2. Electronics set-up showing the different parts and the modules they incorporate. Identical set-ups were used for both detectors. The amplifier (Research Amplifier 2025, Canberra) settings for the 75% detector were as follows: shaping time = 2 μs, gain = 50×0.7, restorer = norm asymmetric, AFT = on. For the 70% detector, the settings were identical except for the gain which was 10×0.8. The timing filter amplifier (Timing Filter Amplifier 2111, Canberra) settings for the 75% detector were as follows: gain = 10×0.2, differential and integral time constants = 50 ns. For the 70% detector only a different gain setting was used, *i.e.* gain = 10×0.5. Canberra 8713S ADCs were used.

lead cylinder and the additional lead shielding between the implantation and decay stations reduced the γ count rate from any possible contamination at the implantation station by about 8 orders of magnitude (at 2.5 MeV). Furthermore, there was no new implantation during the decay measurement periods and, in addition, the cyclotron beam was switched off in order to avoid the overwhelming background caused by the neutrons from the cyclotron beam. The effect of this is illustrated in fig. 1. Additional shielding with boronated paraffin blocks was used to reduce the neutron-induced background. An extra 2 cm lead shielding between the detector and the source reduced the 511 keV annihilation radiation by a factor of 31. In this way, the total count rate in the detector was significantly lowered, thereby decreasing the corresponding count-rate-dependent effects like dead time, pulse pile-up, etc. The intensity of the 2.3 MeV peak was reduced by a factor of 4.5 only.

The electronic chains for both detectors (fig. 2) were almost completely separated from each other in order to allow interception of possible systematic errors in the detection and acquisition processes as well as an independent analysis of the data from both detectors. The time reference for the TDC was a high-precision 10 MHz pulse generator with an accuracy of one part in 10^7. In case of a valid event, both the energy and the time of the event were stored. Because it has been shown before [16] that the simple use of a pulse generator to correct for count losses due to dead time and pulse pile-up is not accurate enough when one needs high precision and/or is dealing with high count rate fluctuations (when measuring during a period of seven half-lives the count rate decreases by two orders of magnitude), a proportional pulse generator, that followed the count rate of the radiation pulses, was used. If the count rate is dominated by a single decay process, as was the case here, the half-life of the pulse generator and the radiation data are equal and both type of pulses undergo the same losses.

Each measurement cycle consisted of about 150 s of implantation and 500 s of decay acquisition. During one cycle all data were written in the RAM computer memory and no hard disk action was allowed in order to prevent extra dead time. About 30 to 40 cycles were organized in one block. Every block was manually started and stopped while sequencing within one block was fully automatic to ensure identical processing for every cycle.

3 Analysis

The raw data were first checked for irregularities and anomalies noted during acquisition and/or visual inspection of the energy and time spectra. Thus, a total of 808 good cycles with a total of $3.6 \cdot 10^6$ counts in the 2.3 MeV γ peak were finally retained for further analysis. A typical energy spectrum of the experiment is given in fig. 3. Here the complete spectrum of the data set for one detector is represented. Detailed analysis of this spectrum revealed the background level in the total recorded energy range to be constant at a level of about 8 counts/channel. The background-to-peak intensity ratio of the pulse generator peak was $5.9 \cdot 10^{-4}$. The contribution to this ratio due to the pile-up of the 2.3 MeV was $2.2 \cdot 10^{-4}$. On average, the total count rate in the germanium detector in the first 10 seconds of the cycle was 550 counts per second.

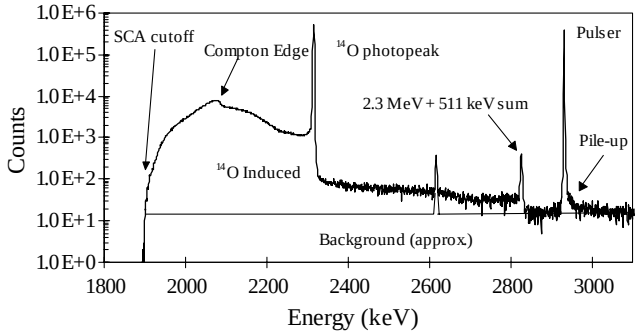

Fig. 3. Total energy spectrum of the data set for detector 1 identifying different peaks and features. The background peak at 2.614 MeV is from the ^{232}Th natural decay chain.

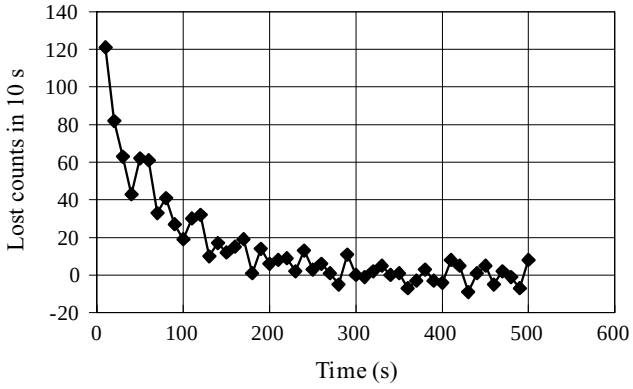

Fig. 4. A typical graph of the evolution of the count losses as a function of the time after the start of the acquisition. The average count loss in the first 10 s amounts to 0.8.

The position and width of the 2.31 MeV γ photopeak and the pulse generator peak were noted and the number of counts in these peaks, as a function of time, was extracted. The peak intensity was not yet corrected for background counts. This correction was performed later on. All these time spectra were then squeezed by a factor of 10, thereby reducing the time spectra to 50 channels of 10 s each in order to make the determination of count-losses and background statistically more significant. The two time spectra resulting from the previous step, namely those for the 2.31 MeV photopeak and the pulse generator peak, together with the pulse counts from the command and pulse count computer, formed the basis for the rest of the analysis. The 2.31 MeV photopeak time spectra yielded the value for the ^{14}O half-life, while the other spectrum was used to apply corrections.

3.1 Count-loss corrections

Because the count losses for which corrections had to be applied (random summing and dead time) are count-rate dependent they affected mainly the statistically most important data points, namely the early time slices. When not corrected, the data would thus yield a longer half-life than the actual one.

As was mentioned already, a proportional pulse generator was used to correct for count losses. The correction was applied for every time slice separately because the count losses are strongly count-rate dependent and thus time dependent. An illustration of this dependency is given in fig. 4. As can be seen, this graph has points with negative values which means a negative count loss. The cause of this was identified as a synchronization problem between the TDC and the pulses-sent counter. However, this offset could be measured indirectly as 217 ± 7 ms and hence the data could be corrected. Due to the statistical nature of the counts in the offset time, this correction induced an error which propagated to the half-life result.

3.2 Background corrections

To determine the background under the γ and pulse generator peak, extensive use was made of the flexibility in analysis provided by the event-by-event mode of the data acquisition. The energy spectra corresponding to the last 10 seconds of the acquisition (that is from 490 s to 500 s after implantation) were used (fig. 5). For these, the ^{14}O signal is reduced by a factor of 123 compared to the signal at the start of the decay measurement. The background, however, stayed constant over the whole period. This "late" energy spectrum had the lowest signal-to-background ratio.

First it was checked that the background indeed stayed approximately constant. For this, the region between the 2.3 MeV photopeak and the pulse generator peak, excluding the 2.8 MeV summation peak, was used. The signal in this region consisted mainly of pile-up counts of the 2.3 MeV photopeak. The time evolution of the events in this region was thus not only caused by the decay of

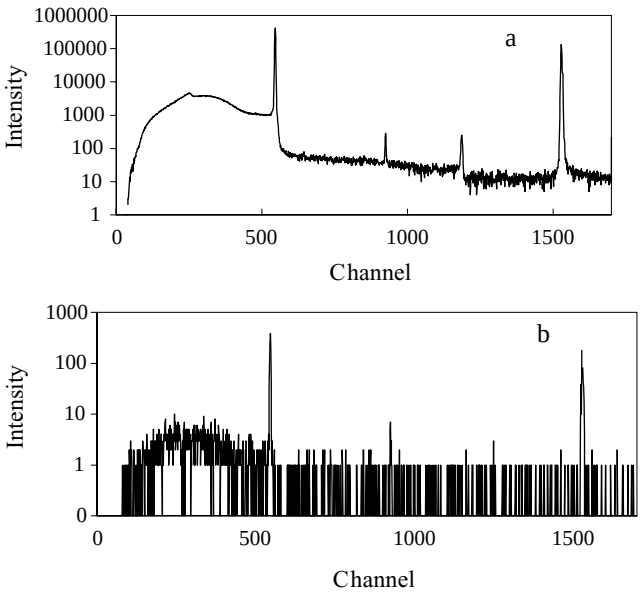

Fig. 5. Two spectra of the same block: a) for 0 to 500 seconds acquisition and b) for 490 to 500 seconds acquisition. See fig. 4 for peak identification.

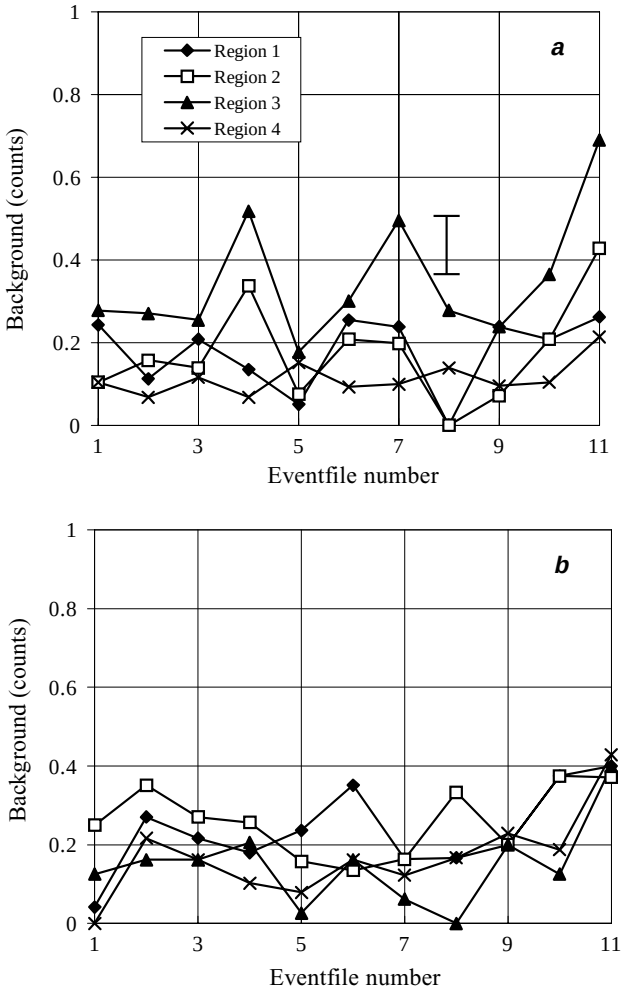

Fig. 6. The evolution of four background regions between the 2.3 MeV peak and the pulse generator peak as a function of time (by increasing event file number) for the total run. a) data set detector 1, b) data set detector 2. In panel a) a typical error on the data points is given. The data are normalised to the total acquisition time.

^{14}O but also by the decrease of pile-up with decreasing count rate. This region was then split into four parts and the counts (mostly background) were compared to the different blocks, providing information on the long-term evolution of the background. The result of these comparisons is shown in fig. 6 for both detectors. It can be seen that, indeed, the background stayed approximately constant throughout the complete run (approx. 77 hours) with no systematic behavior. It is thus justified to extract one background for each detector over the total run. The sensitivity of the half-life to this approximation has been checked and included in the final uncertainty.

The background per channel was determined for every channel between the 2.3 MeV peak and the pulse generator peak using an iterative procedure [11]. The background needed to correct the half-life data was the total

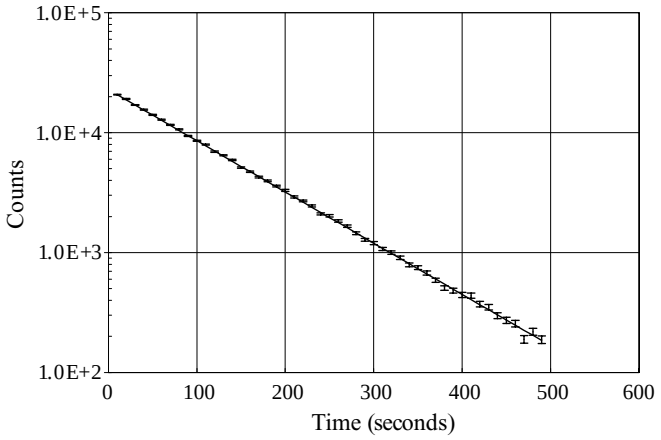

Fig. 7. Example of a fit of one block. The error bars on the data points are given.

background under the 2.3 MeV peak and was obtained by extrapolating the value derived for the high-energy side of the peak. This was done by linear regression of the data points in the assessed region, which yielded 0.303 $\pm$ 0.065 counts/channel/10 s for detector 1 and 0.402 $\pm$ 0.071 counts/channel/10 s for detector 2. There was almost no energy dependency in these mean values (slope always less than $2.4 \cdot 10^{-4}$). It finally appeared that the mean signal over background ratio was about 3600 (detector 2) to 3700 (detector 1). The above-mentioned error bars on the background correction were propagated into the ^{14}O half-life result.

Great care has to be taken when fitting high-precision half-life data. Indeed, the often used method of fitting the logarithm of the data points to a straight line has been shown to introduce a systematic error in the result [17] if an accuracy of 1% or better is aimed for. Therefore, the data have been fitted to a one-component exponential function. The maximum likelihood was used for this, which is justified by the fact that enough statistics remain in each bin, even after 500 seconds. The one-standard deviation error was determined numerically, taking into account the two-dimensional nature of the error space (amplitude + half-life). This fitting of the data was done for each block separately (fig. 7), since every block consisted of an independent measurement. Table 1 gives the summary of the half-lives obtained from each block and the corresponding weighted mean values.

4 Evaluation of the result

4.1 Error caused by count-loss and background corrections

The relative importance of the errors associated with the count-loss and background corrections can be shown as follows. The ratio of the statistical error, the count-loss error and the background error on the intensity in the different time bins is 100/70/0.2 for the first time slices and 100/60/2 for the final ones. The contribution to the

Table 1. Summary of the half-lives and uncertainties of all the blocks for the two detectors. For every block the half-life (in seconds) is given in the left column, while the error is given in the right column (in seconds). Finally, the weighted mean of all values for one data set is given below. A final result of 70.560 ± 0.049 s is obtained.

	Detector 1		Detector 2	
	$T_{1/2}$ (s)	Error (s)	$T_{1/2}$ (s)	Error (s)
1	70.969	0.412	70.240	0.340
2	70.682	0.303	70.611	0.259
3	70.580	0.209	70.671	0.178
4	70.483	0.205	70.510	0.181
5	70.546	0.199	70.580	0.187
6	70.410	0.198	70.398	0.172
7	70.764	0.201	70.446	0.198
8	70.878	0.779	71.064	0.653
9	70.797	0.245	70.532	0.206
10	70.609	0.342	70.992	0.296
11	70.469	0.256	70.358	0.217
Weighted mean	70.597	0.074	70.531	0.066

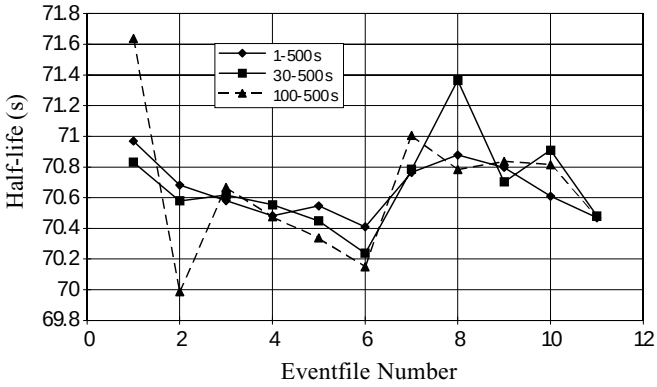

Fig. 8. Dependency of the half-life obtained for the individual event files (detector 1) when different starting bins are used during the fit. The good agreement shows no indication for over- or under-corrected count losses.

total error on the half-life of ^{14}O caused by the background and count-loss corrections amounts to 0.007 s.

4.2 Behaviour of different data parts

If the count-loss corrections, which are strongly dependent on the count rate, were incorrect, meaning that data are over- or under-corrected, the half-life behavior of different time slices should be different. Therefore, all blocks were subjected to fits starting at 1, 30 and 100 seconds into the decay. Any clear systematic behavior of the resulting half-lives could be an indication for incorrect data adjustments. Figure 8 shows the result of this analysis for one data set. For each block in the data set the fitted half-life for the three different decay parts are given. The error bars for the 1–500 s data points can be found in table 1 and are in the range 0.2–0.8 s. The good agreement shows no indication for over- or under-corrected count loss.

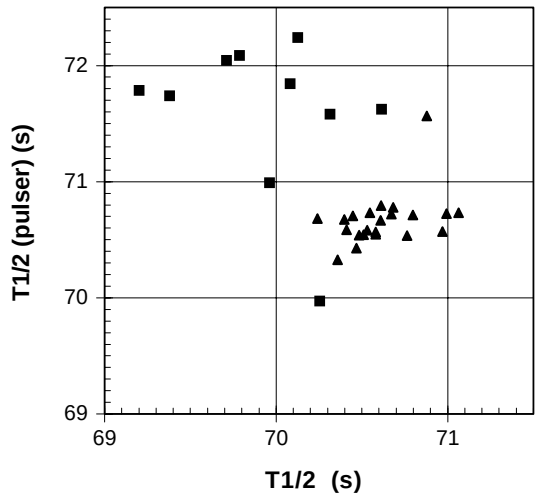

Fig. 9. Correlation plot of the half-life deduced from the 2.3 MeV γ line of ^{14}O and the half-life extracted from the time behavior of the pulser peak. Triangles are for the data of the experiment discussed here. The squares are from a separate experiment where an about 5 % ^{13}N^{14}O contamination was present under the mass 26 peak due to a poor mass resolution when an ECR ion source was used to produce the ^{14}O radioactive source. For clarity, the errors on the half-life are not shown, but these can be found in table 1 (triangles).

4.3 Consistency check and final result

The applied procedure for count-loss correction using the variable pulse generator rate method is only valid [7] if all decaying samples have the same component source strengths or when the pulse generator rate is proportional to the input rate of the one particular species under study. Because of the very low contamination level, these conditions were fulfilled. However a few % contamination could already cause problems. This is checked in fig. 9 (triangles) where, for all blocks, the deduced ^{14}O half-life is plotted *vs.* a half-life determined from the pulser count rate. This "pulser half-life" was obtained by fitting the number of pulses that were sent to the preamplifier of the detector (fig. 2) with a single exponential curve. The data are clearly correlated and grouped together. The average "pulser half-life" (=70.67 s) resembles the ^{14}O half-life, indicating that the total activity detected is due to the decay of ^{14}O. Also, the two data sets give consistent results for the half-life of ^{14}O: $T_{1/2}$ (detector 1) = 70.597 ± 0.074 s, $T_{1/2}$ (detector 2) = 70.531 ± 0.066 s (see table 1). The reduced scattering of the pulser data is due to larger statistics compared to the 2.3 MeV γ-ray intensity. The final result for the half-life of ^{14}O, derived from the two data sets, reveals: $T_{1/2}$ (^{14}O) = 70.560 ± 0.049 s.

For comparison we show in the same figure, fig. 9 (squares), also results from data obtained with a ^{14}O source that was slightly contaminated. An about 5% ^{13}N^{14}O contamination under the mass 26 peak resulted from a poor mass resolution, when using an ECR ion source to produce the ^{14}O radioactive source [11–13]. These data show strong scattering and exhibit a larger "pulser half-life" (= 71.59 s). The latter evidences the

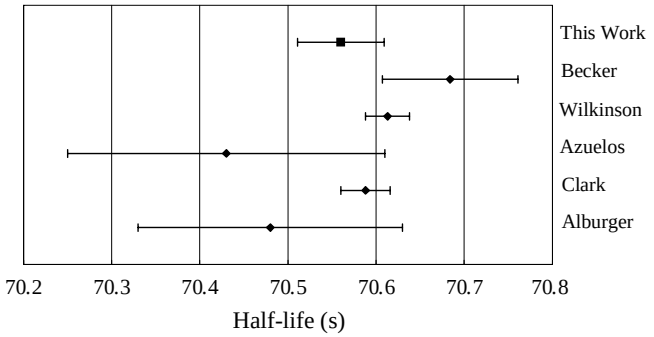

Fig. 10. Summary of all high-precision measurements of the ^{14}O half-life including the value obtained in this work. Data are from Becker *et al.* [8], Wilkinson *et al.* [10], Azuelos *et al.* [7], Clark *et al.* [9] and Alburger [6].

presence of a longer-lived contamination. This would result in an apparent shorter ^{14}O half-life due to the applied correction procedure [7].

5 Comparison with other data and conclusion

Figure 10 compares the five previous high-precision measurements with the new value. The uncertainty on our result is about four times smaller than Alburger [6] and Azuelos *et al.* [7] and also about 1.6 times better than Becker *et al.* [8]. Only Clark *et al.* [9] and Wilkinson *et al.* [10] report an even smaller error bar. Our result is compatible with the adopted mean of 70.603 ± 0.018 s [1,2]. However, by comparing the experimental conditions and the applied correction and analyzing the procedures of the three previous high-precision measurements [8–10] with the experiment reported here, some caution is called for. We discuss these points in some detail now.

5.1 Purity of the radioactive source

It is to be noted that, in contrast to the present measurement, all previous experiments [6–10] have been performed in-beam and thus suffered from possibly strong contamination of longer-lived pure β^+-emitting activities like ^{11}C, ^{13}N and ^{15}O. Contamination levels up to 50% were reported [9]. Therefore all measurements concentrated on detecting the 2.3 MeV characteristic γ-ray of ^{14}O and on the energy selection capability of the different detectors: plastic, NaI and Ge(Li) detectors. A reduction of the 511 keV annihilation radiation, the β^+-radiation and the bremsstrahlung (the main source of pulse summing) was in all cases obtained by placing Pb or Ta shielding between the source and the detector. Furthermore, the source strength was limited so as to reduce the pile-up effects. The count rate (in counts per second) in the first time bin was: < 2500 [9], $\leqslant 1500$ [8], 1500–3200 [10] and only 550 in the present work. Different procedures were applied to correct pulse pile-up. Clark *et al.* [9] and Wilkinson *et al.* [10] checked the influence of pile-up by fitting the data starting from different times, similar to what was described above. However, it should be noted that, due to the limited time interval considered, this procedure is mainly sensitive to random summing with the 511 keV radiation from the decay of ^{14}O and not so much to random summing with the 511 keV radiation from long-lived activity like ^{11}C and ^{13}N. Becker *et al.* [8] determined the amount of pile-up by considering a background window to the right of the 2.3 MeV photopeak with the same width as the photopeak window. From the time behavior of these background counts, they deduced a time-dependent part which they identified as the pile-up part and a time-independent part, which they considered to be the real background. When inspecting for example fig. 3, one notices that the procedure from Becker *et al.* has to be questioned. First of all, the pile-up events are scattered over a much larger energy domain than the one Becker *et al.* considered. Secondly, in view of the longer-lived contaminating activity, the assumption of a time-independent constant background is questionable and the pile-up with the 511 keV radiation from these longer-lived contaminants, which is of the same intensity compared to the 511 keV from ^{14}O, must be present and will influence the final result. Thirdly, part of the counts at the right-hand side of the 2.3 MeV photopeak are due to "true" summing of the 2.3 MeV γ-ray with the 511 keV radiation from the same ^{14}O nucleus. These counts exhibit a pure ^{14}O half-life.

5.2 Peak-to-background ratios

The peak-to-background ratio for the 2.3 MeV γ transition changed considerably over the different experiments and values were about an order of magnitude smaller compared to the present work. The values at the beginning of the time cycle were as follows: 800 [8], 1000 [9], 1250–2000 [10] and 17000 in the present work. Furthermore, as mentioned above, the procedure to obtain the background underneath the 2.3 MeV photopeak by Becker *et al.* [8] can be questioned. In this work we have determined the background using an iterative procedure and have verified its constancy over a wide energy range.

5.3 Dead-time correction

Finally, it should be noted that the dead-time correction procedure used by Becker *et al.* [8] involves a global count-loss correction (due to pulse summing as well as to the dead time of the detector and acquisition system). As they performed a partial correction for the pulse pile-up, using the time-dependent background, they over-corrected the pulse pile-up loss as it was already included in the pulser correction procedure.

6 Conclusion

In conclusion, a new half-life measurement of ^{14}O, using mass-separated samples combined with germanium detec-

tors for the detection of the 2.3 MeV γ-radiation, is presented. This constitutes the first ^{14}O half-life measurement with a mass-separated and virtually contamination-free source. Although the result is compatible with the adopted mean value, this should not be considered as if contamination does not influence the final result. A comparison between the different measurements of the ^{14}O half-life, combined with the information obtained from the γ-ray spectra presented here, shows that the earlier results might indeed have been influenced by the strong source contamination of longer-lived β-decaying nuclei. The good agreement at best indicates that a possible deviation of the previous results from the true value, due to contamination, is of the same order or less than the quoted error bars. The fact that some of the systematic uncertainties in the present work arise from very different factors than those in earlier measurements gives greater confidence that the overall average result (the new mean value, including our result, is 70.597 ± 0.017 s with $\chi^2/\nu = 0.766$) is likely accurate within its error bars. The ^{14}O half-life can, therefore, be considered as a reliable input value for the evaluation of the average ft-value of the superallowed $0^+ \rightarrow 0^+$ Fermi β transitions. Of course, this is only one out of a large number of input values and therefore a continued effort, both experimentally and theoretically, is needed to solve the observed deviation of the value for V_{ud} that is obtained from this average ft-value from the Standard Model. Recent developments at on-line mass separators, for example the implementation of resonant photo-ionization [18], at recoil separators, and other facilities have enlarged the possibilities for the production of intense and pure sources of short-lived radioactive isotopes. In view of these achievements and of the discussion above, new high-statistics half-life measurements should be considered.

We would like to thank Paul Van den Bergh and Johnny Gentens for programming and automation assistance and for operating the mass separator, and the CYCLONE cyclotron crew for delivering excellent beams. M.G. was a fellow of the Belgian IWONL/IWT, M.H. was a research director and N.S. a senior research associate of the FWO-Vlaanderen, Belgium. This work was performed in part with the financial support of the IUAP Research Program of the Belgian State and of the FWO-Vlaanderen, Belgium.

References

1. J.C. Hardy, I.S. Towner, V.T. Koslowsky, E. Hagberg, H. Schmeing, Nucl. Phys. A **509**, 429 (1990).
2. I.S. Towner, J.C. Hardy, *Proceedings of the 5th International WEIN Symposium, Physics beyond the Standard Model, Santa Fe (NM, USA) 1998*, edited by P. Herczeg, C.M. Hoffman, H.V. Klapdor-Kleingrothaus (World Scientific, Singapore, 1999) p. 338.
3. J. Reich et al., Nucl. Instrum. Methods Phys. Res. A **440**, 535 (2000).
4. W.J. Marciano in ref. [2], p. 409.
5. D.H. Wilkinson, Nucl. Instrum. Methods A **335**, 172 (1993).
6. D.E. Alburger, Phys. Rev. C **5**, 274 (1972).
7. G. Azuelos, J.E. Crawford, J.E. Kitching, Phys. Rev. C **9**, 1213 (1974).
8. J.A. Becker, R.A. Chalmers. B.A. Watson, D.H. Wilkinson, Nucl. Instrum. Methods **155**, 211 (1978).
9. G.J. Clark, J.M. Freeman, D.C. Robinson, J.S. Ryder, W.E. Burcham, G.T.A. Squier, Nucl. Phys. A **215**, 429 (1973).
10. D.H. Wilkinson, A. Gallmann, D.E. Alburger, Phys. Rev. C **18**, 401 (1978).
11. M. Gaelens, *Production and use of intense radioactive ion beams:* ^{14}O *as a case study*, Ph.D. thesis, Leuven, 1996 (unpublished).
12. M. Gaelens, P. Decrock, M. Huyse, M. Loiselet, G. Ryckewaert, G. Vancraeynest, P. Van Duppen, *Proceedings of the 11th Workshop on ECR Ion Sources (ECRIS 11) Groningen, 1993*, KVI Internal Report.
13. M. Gaelens, P. Decrock, M. Huyse, P. Van Duppen, M. Loiselet, G. Ryckewaert, Rev. Sci. Instrum. **67**, 1347 (1996).
14. M. Huyse, P. Decrock, P. Dendooven, J. Gentens, G. Vancraeynest, P. Van den Bergh, P. Van Duppen, Nucl. Instrum. Methods B **70**, 50 (1992).
15. R. Kirchner, E. Roeckl, Nucl. Instrum. Methods **133**, 187 (1976).
16. G. Azuelos, J.E. Crawford, J.E. Kitching, Nucl. Instrum. Methods **117**, 233 (1974).
17. D.C. Robinson, Nucl. Instrum. Methods **79**, 65 (1970).
18. Y. Kudryavtsev, J. Andrzjewski, N. Bijnens, S. Franchoo, J. Gentens, M. Huyse, A. Piechaczek, J. Szerypo, I. Reusen, P. Van Duppen, P. Van Den Bergh, L. Vermeeren, J. Wauters, A. Wohr, Nucl. Instrum. Methods B **114**, 350 (1996).